Dynamic Wind Tunnel Tests of the Simulated Shuttle External Cable Trays

K.J. Orlik-Rückemann* and J.G. LaBerge†
National Aeronautical Establishment, National Research Council of Canada, Ontario, Canada

Oscillatory pitching and plunging experiments were performed on models of the cable trays employed on the external tank of the Space Shuttle. The models were mounted transversally to the flow to simulate the significant local cross flows that can be expected as a result of the effects of the bow shock around the nose of the solid rocket booster and the associated flow separation. Several cross sections of the trays were investigated and the surface of the external tank was simulated by a ground plane. The oscillatory experiments were supplemented by some flow visualization studies. Results were obtained over a range of Mach numbers from 0.21 to 0.95 and for a range of angles of attack. It was shown that the large aerodynamic undamping found at certain combinations of these parameters could be eliminated by the use of suitable ramps mounted on the ground plane upstream of the models.

Introduction

LONG trays of approximately rectangular cross section are employed on the external tank of the Space Shuttle to carry various cables from the tank and from the solid rocket boosters to the Orbiter. It was shown, by other investigators, that these trays can be exposed to significant local cross flows with concomitant flow separations and that such flows could, in principle, induce torsional or bending instability of the trays, thereby endangering their structural integrity.

The present wind tunnel study had two purposes. The primary one was to determine the relevant static and dynamic aerodynamic characteristics of the trays in sufficient detail to permit the carrying out of a meaningful aeroelastic analysis of the problem. The secondary purpose was to examine the efficacy of various passive aerodynamic means to eliminate any instability that would be indicated by such an aeroelastic analysis of the initial tray configurations. For various reasons, it was not practical to consider the possibility of the strengthening of the trays or their mountings. The pertinent aeroelastic analysis and the relevant studies of the dynamics of separated flows are discussed by other investigators.[1] This paper is primarily concerned with the dynamic wind tunnel experiments on the simulated model-scale cable trays.

Full-Scale Problem and Its Model-Scale Simulation

The location of the LO_2 and LH_2 cable trays on the external tank of the Space Shuttle is shown in Fig. 1. The off-center location of these trays, toward the right-hand side solid rocket booster (SRB), is clearly visible. Because of this offset location, some segments of the cable trays, particularly the rear segments of the LO_2 cable tray, are exposed to a significant amount of cross flow caused by the SRB bow shock and by the associated flow separation on the external tank in the region of the SRB nose. This effect, already noted in Ref. 2, is also indicated in Fig. 1. The predicted longitudinal distribution of the cross flow over the LO_2 and LH_2 cable trays is shown in Fig. 2 for several Mach numbers (from Ref. 3). As also shown in Fig. 2, the SRB cable trays are located at the rear of the external tank and are perpendicular to the main flow.

All trays are mounted on the external tank by means of fairly rigid supports which, however, are spaced at intervals large enough (33-64 in.) to cause concern over the danger of the occurrence of flow-induced bending or torsional oscillations of the tray segments between the supports. In order to assess the susceptibility of the trays to such potentially destructive behavior, the structural and aerodynamic characteristics of the trays must be available. The aerodynamic information required consists primarily of the two-dimensional characteristics of the trays in a cross flow at a Mach number representative of the cross-flow component of the resulting flow, as shown in Fig. 2, and in the presence of the surface of the external tank. To study the possibility of torsional oscillations, the static and dynamic pitching moment characteristics of a two-dimensional "wing" with the same cross section as the tray and performing an *oscillation in pitch* are needed, while for the study of the possible bending oscillation, the static and dynamic lift characteristics of such a "wing" performing *plunging oscillation* are of interest. Since, for various reasons, the possible instability appeared to be more likely to occur in torsion than in bending, this paper is mainly concerned with the pitching experiments, although some plunging experiments will also be discussed. All experiments were conducted in a high-speed wind tunnel in a Mach number range of 0.21 to 0.95.

The cross sections of the various trays on the external tank have slightly different proportions and different detailed

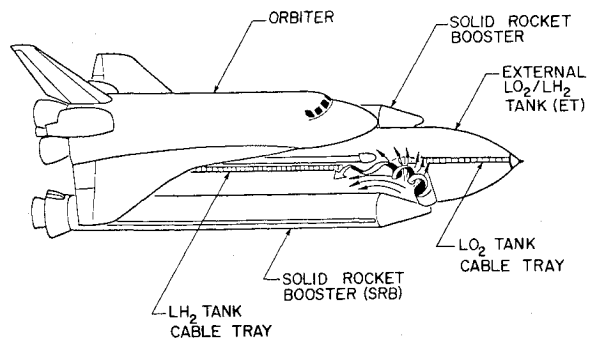

Fig. 1 Location of cable trays on Shuttle launch configuration and SRB-induced cross flow.

Presented as Paper 81-1879 at the AIAA Atmospheric Flight Mechanics Conference, Albuquerque, N. Mex., Aug. 19-21, 1981; submitted Sept. 30, 1981; revision received June 24, 1982.

*Head, Unsteady Aerodynamics Laboratory. Fellow AIAA.
†Research Officer.

outlines, although they all resemble a 2:1 rectangle. Since the LO_2 tray, according to Fig. 2, could be expected to experience more significant cross flow than the LH_2 tray, the cross sections of models 1-4, shown in Fig. 3, were all based on the LO_2 tray geometry. They were all modifications of the basic rectangle, with sharp or rounded-off leading edges (to illustrate limiting cases for corner roundness of the thermoprotection system) and with or without the cutouts typical of the LO_2 tray. (In fact, physically, models 2-4 were all obtained by successive modifications of model 1.) An additional model, of slightly different proportions, was available to simulate the SRB cable trays (model 5). Compared to the actual trays, the scale of all the models was 0.23 to 0.19 (the latter figure applying to model 5 only).

An important feature to be correctly simulated was the presence of the surface of the external tank. Since the tank is very large compared to a cable tray, it was deemed sufficient to simulate the curved (cylindrical) surface of the tank by means of a flat ground plane. The relative distance of that ground plane from the tray was representative of the location of the LO_2 tray relative to the tank surface. The angle between the tray and the ground plane was varied during the investigation, in recognition of the fact that the geometrical angle (slightly positive for the LO_2 tray) would, in reality, be modified, in a manner that was both varying and usually not too well known in advance, by the presence of viscous effects (boundary layer on the tank and on the ground plane).

For practical reasons, the required two-dimensional oscillatory experiments had to be replaced by experiments performed on models with finite span. The models, however, were equipped with suitable root fences and end plates to insure as good a simulation as possible of the desired two-dimensional flow.

Pitching-Oscillation Experiments

The experimental arrangement for pitching-oscillation experiments is shown in Fig. 4. The model was elastically mounted in a half-model oscillatory apparatus, located outside the wind tunnel wall. A pair of the lightweight coils moving in a magnetic field and a cruciform spring provided the electromagnetic excitation and the restoring moment in pitch, respectively. The model was attached to the spring by means of an adapter (integral with the model) that passed through both the wind tunnel wall and a circular reflection plate, the latter being used to reduce the effect of the wind tunnel wall boundary layer. The ground plane (GP), simulating the tank surface, and a cylindrical bar, simulating a pipe on the tank, were mounted directly on the reflection plate. The ground plane and the cylindrical bar were always used together. The angle of attack of the model was adjustable in such a way that the ground plane remained always parallel to the flow. The span of the ground plane was slightly larger than that of the model and its distance from the model could be varied. All experiments were performed in the National Aeronautical Establishment (NAE) 30×16 in. suction wind tunnel at Mach numbers ranging from 0.21 to 0.95, with the corresponding Reynolds numbers varying from 4.5 to 15×10^6/m. A photograph of the experimental arrangement is shown in Fig. 5.

Unless otherwise indicated, all the pitching-oscillation experiments were performed with an oscillation amplitude of 1.25 deg and at a frequency of 32 Hz. That frequency was low enough to avoid any coupling with the third subharmonic of the Karman vortex shedding,[4] that could invalidate the results.

The pitching moment coefficient C_m, the static pitching moment derivative $C_{m\alpha}$, and the damping-in-pitch derivative $(C_{mq}+C_{m\dot{\alpha}})$ were obtained from the measured instantaneous values of the model angular position, the driving torque, and the oscillation frequency, using standard NAE procedures. The data processing system is fully digital, incorporates a minicomputer, and provides smoothing of the raw data by means of a time-domain analysis that employs cross-correlation techniques.[5]

The oscillatory apparatus was *dynamically* calibrated by replacing the model by a suitable calibrating frame and by simulating the oscillatory aerodynamic reactions acting on the model by accurately known, electromagnetically induced, *alternating* loads, whose phase and amplitude could be adjusted at will. A comparison between the calibration loads

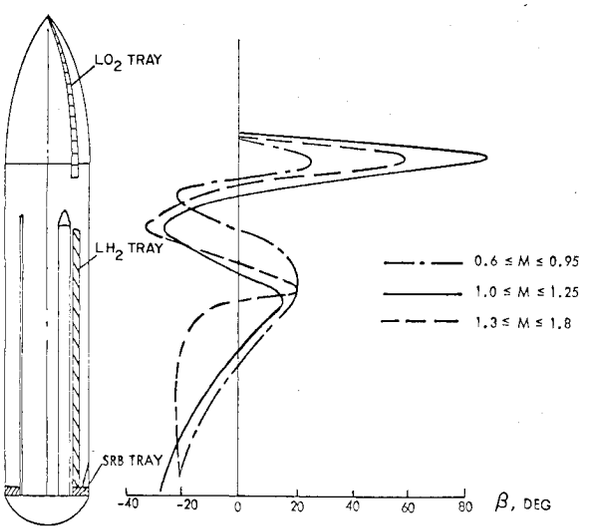

Fig. 2 Predicted cross-flow distribution at cable tray location on ET.

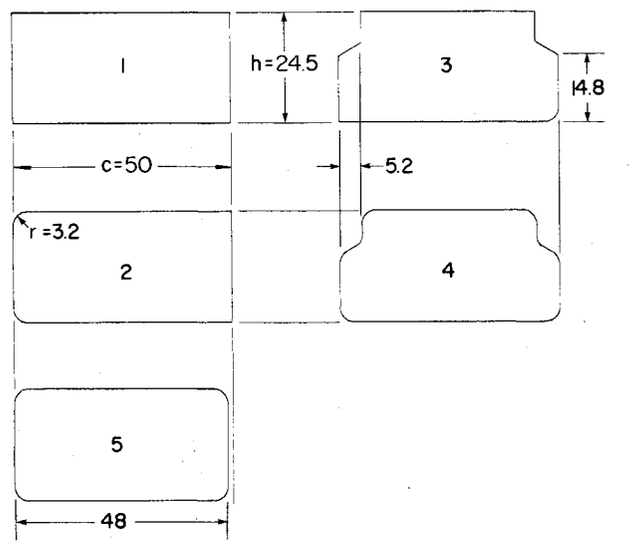

Fig. 3 Cross sections of models used in study (all dimensions in millimeters).

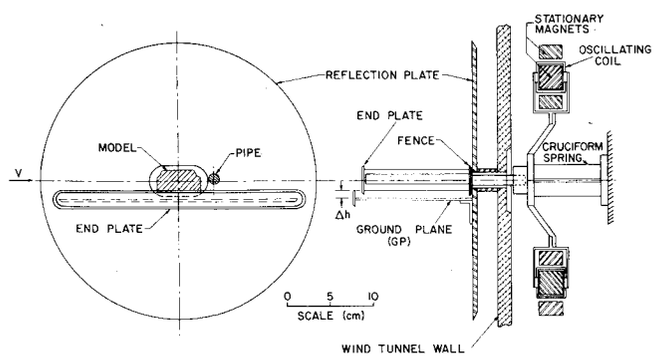

Fig. 4 Experimental arrangement for pitching oscillation experiments.

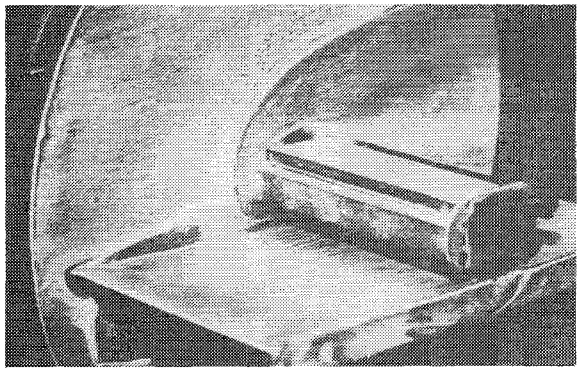

Fig. 5 Experimental arrangement in NAE wind tunnel.

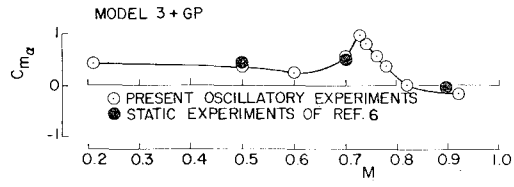

Fig. 6 Comparison of $C_{m\alpha}$ measured in static and dynamic tests.

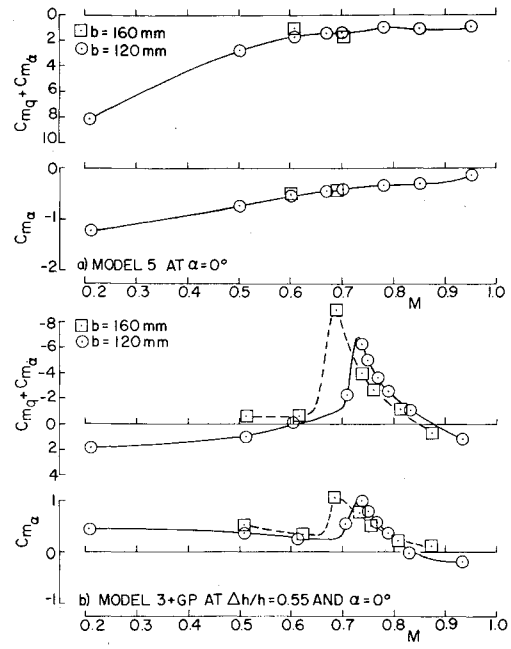

Fig. 7 Effect of span on pitching moment derivatives.

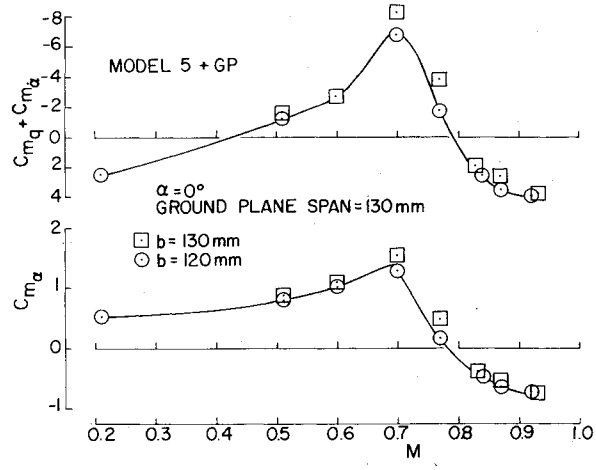

Fig. 8 Effect of the different spans of the model and the ground plane ($\Delta h/h = 0.55$).

and the outputs of the oscillatory apparatus, obtained by processing all of the data by means of the same procedures as during the wind tunnel experiment, provided an overall calibration of the technique and of all the mechanical and electronic subsystems involved.

Although, as mentioned previously, the experiments were not, strictly speaking, two-dimensional, in most cases they represented two-dimensional flow conditions quite well. This can be seen from Fig. 6, where a comparison is shown between the static pitching moment derivative obtained for model 3 (in the presence of the ground plane) in the present investigation and the corresponding results in Ref. 6. Similar conclusions can also be reached by comparing the static and dynamic results obtained with models of different span (Fig. 7a). However, in cases where sudden changes of a derivative with the Mach number occurred, the lack of strict two-dimensionality could sometimes cause a slight shift in the Mach number, at which such a change would occur (Fig. 7b). Smaller deviations from two-dimensional flow, such as can be seen in some of the flow-visualization photographs, did not seem to affect the measured derivatives to any significant degree.

For experiments in the presence of the ground plane, there was some concern over the fact that, in most cases, due to the geometrical requirements of the desired test conditions, the two spans could not be made equal (since the two end plates would then touch). Model 5 was, therefore, tested with two spans ($b = 130$ and 120 mm), one coinciding with the span of the ground plane and one slightly shorter, representing the majority of the test conditions. It can be seen from Fig. 8 that the results are quite close, showing only a slight Mach number shift, as discussed above, in the region of $M = 0.7$.

Pitching Oscillation Experiments—Results

Both the dynamic and the static pitching moment derivatives for the basic rectangular model with sharp edges (model 1) are very small and remain almost constant over the Mach range investigated (Fig. 9), indicating that the flow is probably entirely separated on both sides of the model. By contrast, the rounding off of the leading edges (model 2, $r/c = 0.065$) can be seen, at lower Mach numbers, to be strongly dynamically destabilizing and statically stabilizing, probably due to the flow reattachment at the rear part of the model. As the Mach number increases, however, there is an increase in the negative damping followed, at $M = 0.65$, by a sudden switch to a slightly positive damping, and later to a slightly negative damping again. These changes are probably associated with the appearance of the local shock waves near the leading edge of the model and the confinement of the separated region to an area immediately downstream of the leading edge.

The comparison of the results obtained at $M = 0.7$ for models 1 and 2 is presented in Fig. 10 for a range of angle of attack. The two sets of curves are almost identical and provide a striking example of the close relationship between the statically stabilizing and the dynamically destabilizing (or vice versa) aerodynamic effects on oscillating models in the presence of flow separation and flowfield time lag.

The introduction of a shoulder nick (model 3) on the sharp-edged basic model (model 1) increases the damping at $\alpha = 0$ deg over most of the Mach number range investigated (Fig. 11a) and increases the absolute value of damping at $M = 0.7$ at angles of attack up to 10 deg (Fig. 11b). The effect of a shoulder nick is, however, quite different when the edges are rounded off. At zero angle of attack the large negative damping occurring on model 2 at Mach numbers up to 0.65 is

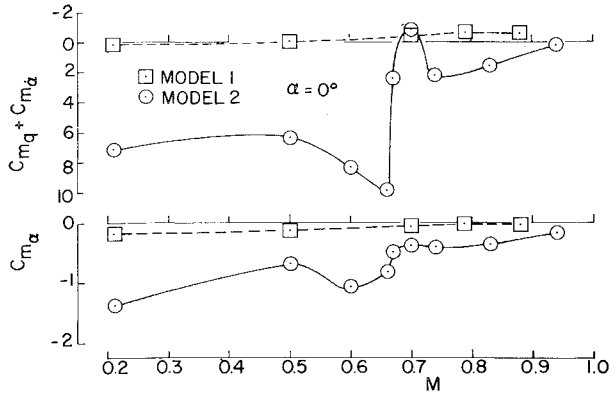

Fig. 9 Effect of rounding off the leading edges of the basic rectangular model, $\alpha = 0$ deg ($b = 160$ mm).

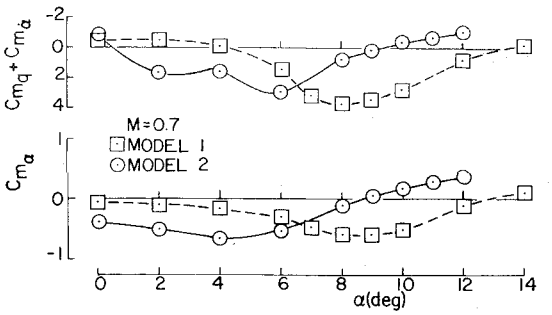

Fig. 10 Effect of rounding off the leading edges of the basic rectangular model, $M = 0.7$ ($b = 160$ mm).

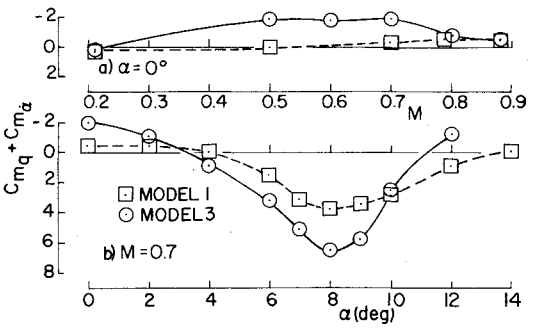

Fig. 11 Effect of shoulder nicks on sharp-edged models ($b = 160$ mm).

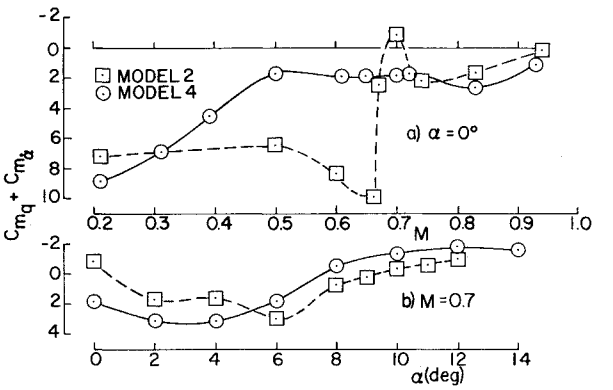

Fig. 12 Effect of shoulder nicks on models with round leading edges ($b = 160$ mm).

greatly reduced on model 4 (except at $M = 0.2$) (Fig. 12a), possibly by the partial reattachment of the flow on the top of the model. At $M = 0.7$, the shoulder nick is dynamically destabilizing at $\alpha \leq 5$ deg and stabilizing at higher angles of attack (Fig. 12b).

The effect of the ground plane (GP) was investigated only for the models with the shoulder nick and is illustrated in Figs. 13 and 14. For both the sharp- and round-edged models, a large increase in the pitch damping occurs at a Mach number around 0.6; this increase is probably related, as discussed in considerable detail in Ref. 3, to the onset of an inlet-type flow between the model and the ground plane, with a shock wave system across the gap (Fig. 15). Specifically, the sudden merger of the two shocks at $\alpha = 0$ deg into one at $\alpha = 2$ deg (Fig. 15) is probably responsible for the local undamping peak at these conditions (Fig. 16). In the round-edged case (model 4), this effect occurs much more gradually than in the sharp-edged case (model 3). As the Mach number increases above 0.7, this is followed, in both cases, by a gradual decrease in damping leading, at $M \simeq 0.85$, to the occurrence of negative damping; this may be associated with the gradual movement of the shocks in the gap between the ground plane and the model.

On the sharp-edged model with the shoulder nick (model 3), the damping is strongly affected by the angle between the model and the ground plane (with the latter aligned with the flow). A well-defined peak of negative damping occurs at $\alpha = -2$ deg at $M = 0.7$ and at $\alpha = 1$ deg at $M = 0.92$ (Fig. 16). Not surprisingly, the peak is much less pronounced when the oscillation amplitude is doubled; however, there is no noticeable effect of frequency (Fig. 16b). No similar well-defined peaks of negative damping have been observed on the corresponding model with round edges (model 4).

The experiments on model 4 in the presence of the ground plane (which was the configuration that most closely resembled the flow around the LO_2 cable tray) clearly showed that a large aerodynamic undamping existed at both the low end (0.2-0.5) and the high end (0.8-0.95) of the Mach number range investigated. It was possible, therefore, that an aeroelastic analysis would indeed find a potential torsional instability problem at those conditions. Various passive aerodynamic "fixes" were, therefore, investigated (Fig. 17) in order to eliminate this undesirable aerodynamic undamping and, therefore, remove the cause of such a possible instability. Two of the "fixes" were found quite effective in suppressing the aerodynamic undamping. In Fig. 18 both the static and dynamic pitching moment derivatives are shown reduced to practically zero in the entire Mach number range investigated by applying a 20 deg ramp (fix W) in front of model 4. This particular fix was later used along the critical portion of the LO_2 cable tray on the external tank used for the first four flights of the Space Shuttle.

Although models 2 and 5 were quite similar, unexpected large differences were obtained in the measured values of the pitch damping, especially at Mach numbers between 0.5 and 0.66 (Fig. 19). A subsequent visualization of the flow on the stationary models has revealed that at Mach 0.6 the flow on model 2 reattaches very near the trailing edge and then moves forward in an almost two-dimensional fashion, while at the same Mach number the flow reattachment on model 5 (with the 4% smaller chord) just "misses" the trailing edge with the result that the resulting reversed flow becomes strongly three-dimensional. The same strongly three-dimensional pattern was exhibited at higher Mach numbers on both models. Flow patterns obtained with partly the regular end plate and partly with one twice as long and twice as high were similar, indicating that the three-dimensionality of the reversed flow is probably a characteristic of the flow separation rather than a result of the experimental setup.

Plunging-Oscillation Experiments

By replacing the cruciform spring in the half-model oscillatory apparatus by a double-cantilever spring, and by reconnecting the coils to move in the same rather than in the

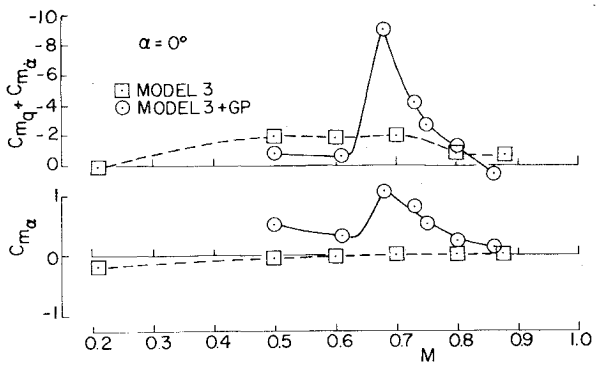

Fig. 13 Effect of ground plane on model 3 ($b = 160$ mm, $\Delta h/h = 0.55$).

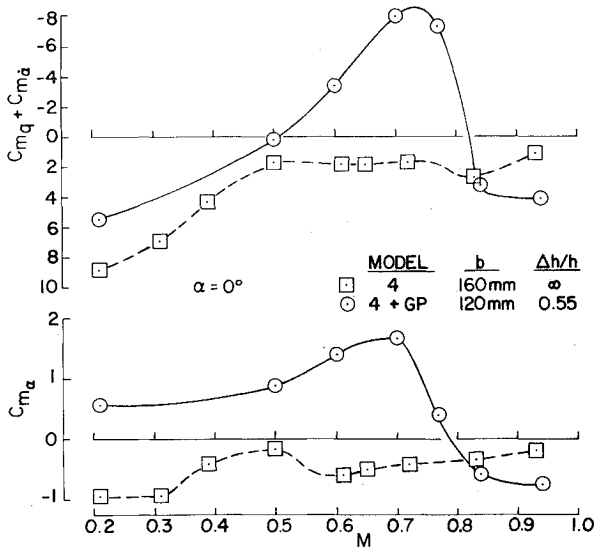

Fig. 14 Effect of ground plane on model 4.

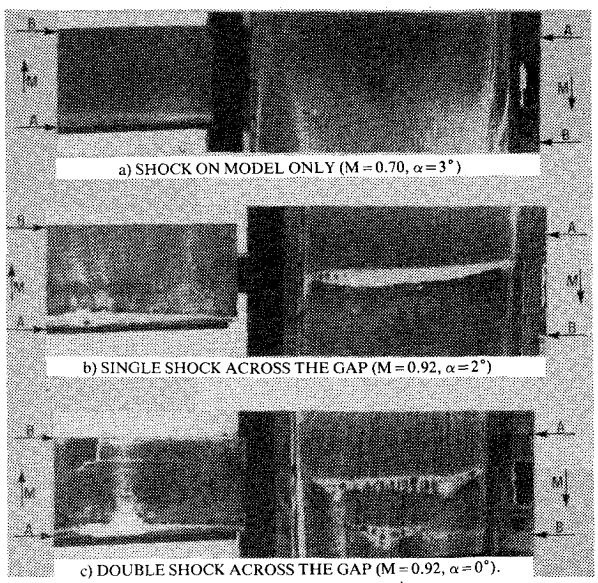

Fig. 15 Oil visualization of flow between model 3 and ground plane.

opposite directions, the equipment shown in Fig. 4 was adapted for performing plunging oscillation. As mentioned previously, this type of experiment is needed to provide the aerodynamic information required to perform an aeroelastic analysis of a possible instability in bending. Since this type of

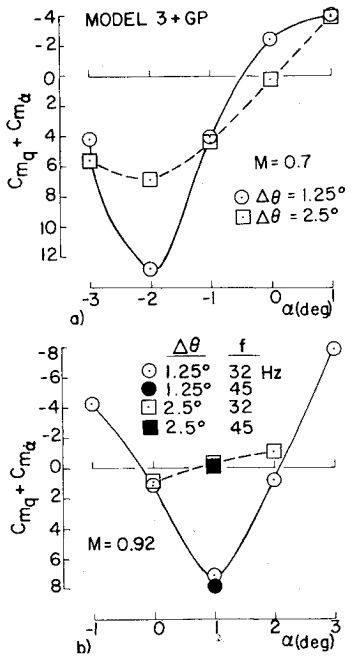

Fig. 16 Effects of incidence, amplitude, and frequency on model 3 with ground plane ($b = 120$ mm, $\Delta h/h = 0.55$).

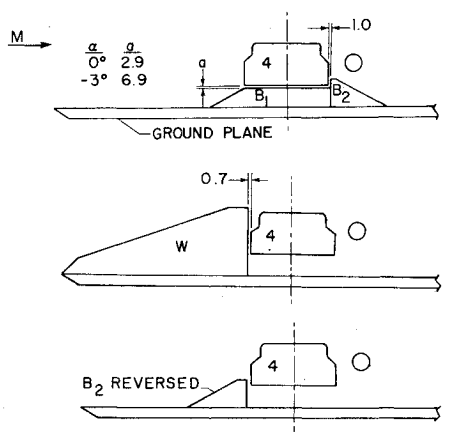

Fig. 17 Passive aerodynamic fixes investigated ($b = 120$ mm).

instability was thought less likely to occur than the previously discussed instability in torsion, only a few plunging experiments were performed.

The plunge-damping derivative $C_{Z\dot{z}}$ for models 3 and 4, with and without the ground plane, is shown in Fig. 20. It can be seen that for both models the presence of the ground plane is highly stabilizing, resulting in good positive damping. It should be noted that because of various separation-induced unsteady effects, the damping derivative for these models can be expected to be quite different from the steady normal-force slope, $C_{Z\alpha}$. In particular, this is true for experiments in the presence of the ground plane. It is therefore necessary to perform plunging experiments to provide reliable data of this kind.

For comparison, an additional point measured on a 17% thick biconvex wing ($b = 140$ mm) is included in Fig. 20. The value shown, $C_{Z\dot{z}} = -3.83$ is very close to $C_{Z\dot{z}} = -3.84$ measured on an NACA 0012 profile at a Mach number slightly above 0.1 and at a similar reduced frequency.[7] The corresponding prediction of the linearized unsteady ($k = 0.14$) wing theory is $C_{Z\dot{z}} = -5.15$.

Additional experimental data and flow visualization photographs can be found in Ref. 8.

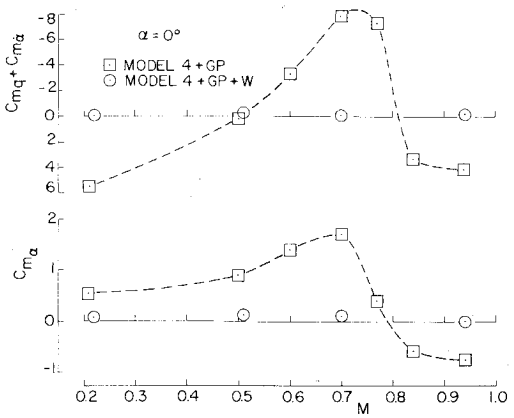

Fig. 18 Effect of fix "W" on model 4 with ground plane ($b = 120$ mm, $\Delta h/h = 0.55$).

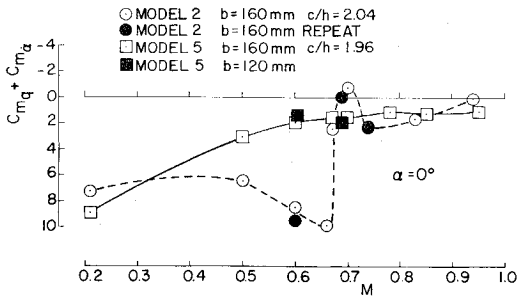

Fig. 19 Effect of model chord/height ratio on pitch damping.

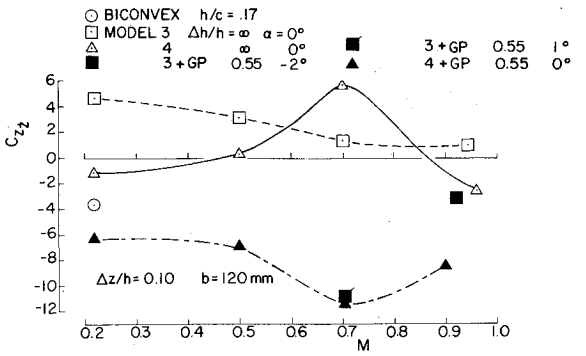

Fig. 20 Plunge damping of models 3 and 4.

Summary and Conclusions

Oscillatory pitching and plunging experiments were performed on transversally mounted models of the Shuttle external tank cable trays to simulate their dynamic behavior in torsion and in bending when exposed to existing local cross flows. It was found that in certain conditions a large aerodynamic undamping in pitch could occur and that such an undamping could be entirely eliminated by installing suitable ramps upstream of the models on the ground plane which simulated the surface of the external tank. One of these ramps was subsequently installed on the external tanks used for the first four flights of the Space Shuttle.

Acknowledgment

This work was performed for Martin Marietta Aerospace under Contract AS9-7514-83.

References

[1] Reding, J.P. and Ericsson, L.E., "Analysis of Static and Dynamic Wind Tunnel Tests of the Shuttle Cable Trays," *Journal of Spacecraft and Rockets*, to be published.

[2] Reding, J.P. and Ericsson, L.E., "Unsteady Aerodynamic Analysis of Space Shuttle Vehicles. Part III, Booster Interference Effects," NASA CR-120124, Aug. 1973.

[3] Ericsson, L.E. and Reding, J.P., "Aeroelastic Analysis of the Shuttle External Tank Cable Trays," LMSC Rept. D766543, Contract ASO-751485, April 1981.

[4] Ericsson, L.E., "Karman Vortex Shedding and the Effect of Body Motion," *AIAA Journal*, Vol. 18, Sept. 1980, pp. 935-944.

[5] Foster, L.R. and Hanff, E.S., "A Second Generation Instrumentation System for Measuring Cross Coupling Derivatives," 8th International Congress on Instrumentation in Aerospace Simulation Facilities, Monterey, Calif., Sept. 1979, *ICIASF'79 RECORD*, pp. 251-256.

[6] Michna, P.J. and Parker, D.R., "Test Results from the Pressure Test of a 0.12 Scale Model of the External Tank LO_2 Cable Tray and GO_2 Pressure Line and a 0.1575 Scale Model of the Aft ET/SRB Cable Tray in the MSFC 14 Inch Trisonic Wind Tunnel Test No. TWT 661," Martin-Marietta Corp., Michoud Operations, New Orleans, La., Report MMC-ET-SEO5-89, May 1980.

[7] Halfman, R.L. "Experimental Aerodynamic Derivatives of a Sinusoidally Oscillating Airfoil in Two-Dimensional Flow," NACA TN 2465, 1951.

[8] LaBerge, J.G., "Dynamic Wind Tunnel Tests of the Shuttle External Tank Cable Trays at Subsonic Speeds," NRC NAE LTR-UA-55, Feb. 1981.